Thermophysical properties of Choline and Pyridinium based Ionic Liquids as advanced materials for energy applications

J. J. Parajó[1], M. Villanueva*[1], J. Troncoso[2], J. Salgado[1]

[1]NAFOMAT Group. Department of Applied Physics. Universidade de Santiago de Compostela. 15782 Santiago de Compostela. Spain

[2]Thermophysics Laboratory, Applied Physic Department. Universidade de Vigo, Ed. Manuel Martínez Risco campus As Lagoas, 32004 Ourense, Spain

*Corresponding author: maria.villanueva@usc.es

Abstract

Phase transitions, isobaric heat capacities and thermal stability of four ionic liquids (ILs) are determined in this work. The selected ILs have two different cations, pyridinium and choline, and they are combined with three different anions, acetate, dihydrogen phosphate and tosylate. Solid-solid and solid-liquid phase transitions and isobaric molar heat capacities are determined using two calorimeters, both based on the differential scanning calorimetry methodology. Thermal stability of the studied compounds is analysed through the thermogravimetric technique (TGA). Degradation temperatures are obtained from TGA experiments using the dynamic method, whereas isothermal TGA is used to determine the maximum operation temperature. The results show that, all the ILs present crystalline behaviour, with melting temperatures within the interval of 88ºC and 123ºC, whereas heat capacities linearly increases with temperature. A clear dependence with the anion is observed for both heat capacities and thermal stability, being ILs with the tosylate anion those presenting the highest values of molar heat capacities and the highest thermal stability.

Keywords:

Ionic liquid, Liquid range, Maximum operation temperature, Isobaric heat capacity

Introduction

Ionic Liquids (ILs) constitute innovative fluids for chemical processes that are generally non-flammable and non-volatile in environmental conditions. ILs have emerged as an important tool to replace traditional solvents, often improving the process performance and minimizing the environmental impact. The number of ILs and their potential applications has been increased during the last years, as the literature reveals [1–4], although the main part of the published papers are addressed to two general groups: biotechnological and energy applications.

Conventional ILs, mainly imidazolium based ILs, could become part of sustainable products and processes due to their excellent technological properties, but they could be toxic for most organisms, in spite of these fluids are considered green solvents [5]. In this context, novel ILs derivate from natural products opened a new direction in IL design. One possibility is the choline based ILs, which, during last decade, have been involved in relevant studies as, for example, extractants of saponins and polyphenols from mate and tea [6], recombinant human therapeutic protein used for treating advanced melanoma [7], additives in pharmaceutical products [8–10], improvers of crystallization of biopolymers with use on suture, bone fixation material, drug delivery, and tissue engineering [11], antimicrobial agents [12], additives for lubricants [13] or green surfactants [14]. The presence of choline cation in an IL shows multiple advantages, namely good water solubility, non-toxicity, biodegradability and low cost. Another interesting property is that it can be obtained from natural resources; it is found in a wide variety of foods and it has been recognized as an essential nutrient by the Institute of Medicine (IOM) in 1998 [15,16].

Furthermore, the applicability on the energy field of pure choline ILs and as a part of deep eutectic solvents (DES) is also pointed out in early studies. Thus, Zhao *et al.* [17] highlighted the importance of the DES of choline acetate and choline chloride with glycerol in the biodiesel synthesis. Zhang *et al.* [18] emphasised the potentiality of choline ILs as green and cheap agents on cellulose pre-treatment. In a previous work of our group in collaboration with researchers of University of Vigo, Sanchez *et al.* [19] analysed some thermophysical properties as density, viscosity and electrical

conductivity of choline and pyridinium ILs to be proposed as absorbents with water as refrigerant in novel heat pump devices. Furthermore, Ali Rana *et al.* [20] found an increase on the ionic conductivity by up to three orders of magnitude adding choline dihydrogen phosphate to organic ionic plastic crystal matrix in acidic conditions, being an important progress on electrochemical device applications, batteries, electrochromics and fuel cells, for example. This interest as potential electrolytes was also pointed out by other authors [21,22]. Therefore, the future of ILs as advanced materials in the energy field is unquestionable. In these energy applications, the knowledge of liquid range and heat capacities as a function of temperature, among other properties, is of essential importance. This work proposes a new step on the field of ionic liquids as smart materials in energy applications. Both properties, liquid range and heat capacity, for four ILs, three choline based ILs and one ethyl-pyridinium, are here analysed.Three different anions, corresponding to the three IL groups proposed by Gadilohar and Shankarling [8] according to its acidity-basicity, have been chosen: anion acetate belongs to the "basic cations and anions" group; tosylate to the "neutral cations and anions" group and dihydrogen phosphate to the "amphoteric anions" group.

Materials and Methods.

Chemicals

Four ionic liquids, provided by IoLiTec, are considered in this work, three of them with the common cation choline $[Chol]^+$, and the anions Acetate, $[Ac]^-$, Tosylate, $[Tos]^-$ and Dihydrogen phosphate $[H_2PO_4]^-$, and the other one is 1-ethylpyridinium tosylate, $[C_2Py][Tos]$. Identification names, CAS numbers, initial purities and cations and anions chemical structures are presented in Table 1. Water contents were determined by Karl Fischer titration, firstly for samples as supplied. Further purifications were done for heat capacities determinations to ensure that the water content was lower than 200 ppm.

Table 1. Structure, identification, molar mass, mass fraction purity and initial water content of selected ILs (supplied by IoLiTec).

Name	**Abbreviation CAS Number**	**Chemical structure**	**Molecular mass** /g mol^{-1}	**Mass fraction Purity***	**Water content / wt%**
Choline Dihydrogenphosphate	[Chol][H_2PO_4] 83846-92-8	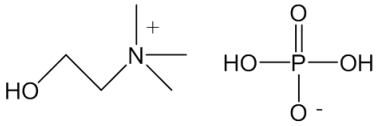	201.16	0.98	0.41
Choline Tosylate	[Chol][Tos] 55357-38-5	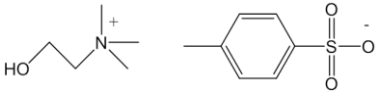	275.36	0.97	0.37
Choline Acetate	[Chol][Ac] 14586-35-7	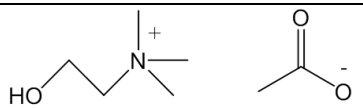	163.21	0.98	2.1
1-ethylpyridinium Tosylate	[C_2Py][Tos] 95982-69-7	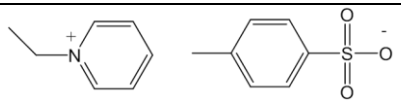	279.36	0.97	0.32

* Determined by NMR in all ILs (supplier indication)

Experimental section

Phase transitions determination

A differential scanning calorimeter DSC Q100 from TA-Instruments with aluminium pans hermetically sealed was used to determine the different phase transitions experimented by the IL during heating and cooling cycles. Samples, without further purification, were placed in a 40-μL hermetically sealed aluminium pan with a pinhole at the top of the cover. An empty aluminium pan was used as reference. Each sample (3 - 5 mg) was subjected to four ramps, two in cooling and two in heating mode, with an isothermal step between them: (a) heating from (25 to 125) ºC at 10 ºC min^{-1}, (b) isothermal step at 120 ºC during 45 minutes in order to remove impurities and to reduce or eliminate free water in sample and to erase the sample thermal history , (c) cooling from (125 to −85) ºC at 10 ºC min^{-1}, (d) isothermal step at -85 ºC during 5 minutes and (d) heating from (-85 to 100) ºC at 10 ºC min^{-1} and (e) cooling from (100 to -85) ºC at 5 ºC min^{-1}. Although a comparison between the cycles at different temperatures was done, transition temperatures were determined from the DSC curves, as the onset points of the different peaks, during the reheating and recooling steps, as it was done in previous papers [23,24].

Heat capacities measurements

Isobaric molar heat capacities were determined using a micro DSC III calorimeter from Setaram. Due to the solid nature of the sample, batch cells with an internal volume around 0.8 ml were used. The scanning method with a heating rate of 0.25 $K \cdot min^{-1}$, was used, obtaining data in the temperature interval (293.15- 348.15) K. Two reference fluids are needed for performing the calibration; toluene and water were selected due to the high precision of the available literature data [25]. Before measurements, samples were dried in vacuum pump during 48h and water content was then measured by Karl-Fisher titration obtaining values lower than 200 ppm. Although this apparatus can determine heat capacity with uncertainty below 1% for high purity compounds, the special hygroscopic nature of the studied ionic liquids worsens the reliability of the measurements in the solid phase. This is mainly because water strongly affects the melting point of these chemicals, making it to not take place at one temperature, but in a temperature interval. Therefore, in the proximity of the melting point, heat capacity data are less reliable. Taking this into account, standard uncertainties of 2% are estimated.

Thermal stability study

Thermogravimetric analysis, in dynamic and isothermal modes under nitrogen and dry air atmospheres, have been performed using a TGA 7-Perkin Elmer. The short-term thermal stability was studied firstly from dynamic scans from (100 to 800) ºC, with a heating rate of 10 ºC min^{-1} and a purge gas flow of 20 cm^3 min^{-1}. Samples of (3-5) mg were placed in an open platinum pan. Each analysis was repeated three times. The atmosphere influence was analysed for all the ILs. Furthermore, isothermal TG analysis at temperatures lower than t_{onset}, was used to determine the long-term thermal stability of ILs. Details about these determination procedures were described in previous papers [26,27].

Results and Discussion

Phase transition analysis

Choline based ILs present similar DSC thermal profiles for the different scanning rates used in this study (10 and 5 ºC min^{-1}). The DSC curves corresponding to the last heating and cooling steps performed at 5 ºC min^{-1} are presented in Fig 1. However, [C_2Py][Tos] shows differences between the DSC profiles at different heating rates (Fig 2). This could be due to the highest rate does not allow the formation of crystalline lattice on cooling ramp at and then, glass transition is observed in heating ramp at -33 ºC, followed by a cold crystallization process (exothermic peak) at -3 ºC, a solid-solid transition (endothermic peak) at 37 ºC and finally a melting (endothermic peak) at 97 ºC. The reduction on scan rate down to 5 ºC min^{-1} induces the appearance of an exothermic peak in cooling ramp, compatible with crystallization, and the disappearance of the glass transition. Therefore, the lowest scan rate induces the reduction of the sample amorphous phase, although a small exothermic peak associated to cold crystallization is observed also for 5 ºC min^{-1}.

The obtained results from these DSC traces, bibliographic data of melting, freezing and glass transition temperatures, as well as the enthalpy and entropy changes of melting of the selected ILs, calculated directly from peak integration and from $\Delta S_m = \Delta H_m/T_m$, respectively, are summarized in Table 2. Despite the scarce and discrepant bibliographic

information about the transitions of these ILs the obtained results are in good concordance with some of the previously published data, as it can be seen in Table 2.

[Chol][Tos] shows melting and freezing peaks at heating and cooling ramps respectively, in addition to solid-solid transitions in both ramps, without any sign of amorphous phases. This melting temperature is in very good agreement with Wandelt and Heilner [28] who reported, in a patent, melting temperatures of 107 ºC.

No evidence of amorphous phase has been observed for [Chol][Ac], which shows melting (on heating ramp) and freezing (on cooling ramp) peaks with onset temperatures at (86 and 59) ºC, respectively. These results are in relatively good agreement with the melting temperature reported by Petkovic *et al.* [29] , Zhang *et al.* [18], Koda *et al*.[30], Muhammad *et al*. [21] and Brünig *et al.* [31] although our results are higher than those reported by Fukaya *et al*. [22].

[C_2Py][Tos] shows strong supercooling, with freezing points significantly lower than the melting points, being the difference $(T_m–T_f)$ up to 90 ºC in the experiment performed at 5 ºC min^{-1}. Interestingly, in a previous work [32] we found that $[C_2Py]^+$ based ILs also presented the largest super cooling effect from a list of ILs with different cation and different anions. As we pointed out in that work, this fact is very important and a useful property for an eventual application of ionic liquids as absorbents in absorption heat pumps, since the problem of crystallisation commonly observed in the current working pairs is avoided.

It is especially interesting the available data of melting point of [Chol][H_2PO_4]; in spite of the DSC curves obtained from different authors are in extremely good concordance, corresponding melting points range between (119 and 190) ºC. The reason is that some authors [33–35] attribute the melting process to the peak appeared around 120 ºC and other authors [11,36] indicate that peak at 120 ºC is due to a solid-solid transitions and the melting corresponds to a small peak around 190 ºC. To clarify this controversial fact, we extended the temperature interval of the first scans to 220 ºC (see Fig S1 in ESI) and an unfinished peak, starting at 180 ºC, was observed at the end of the heating ramp. Taking into account the degradation temperature of this compound, very close to 180 ºC, -see Thermogravimetric analysis subsection of Results section of this work-, the increasing of the upper limit of thermal scan without risk of degradation of the sample was not possible. Therefore, we tried to found visual evidences of the physical state at

temperatures between (120 and 190) ºC; few grams of pure IL were placed into a furnace previously heated at 140 ºC during a couple of minutes and we have observed that the sample started to melt and flow (see Fig. S2 in ESI). After these evidences, the conclusion of the present work is that the peak registered at 120 ºC corresponds to the melting of [Chol][H_2PO_4]. Therefore, the previously observed peak at 180 ºC must be due to the IL degradation process.

Due to the melting temperatures of the selected ILs are relatively high, these compounds should be named molten salts rather ionic liquids if the classical definition is admitted. Some authors [37] refers to this IL as to a near-IL, because is liquid at room temperature when diluted with 20% (v/v) H_2O.

As it was previously indicated, from melting temperatures and enthalpy changes corresponding to this transition, entropy changes included in Table 2 have been calculated. Two important characteristics of plastic crystals are their very low entropies of melting (<20 J mol^{-1} K^{-1}) and the exhibition of a series of solid-solid phase transitions below the melting point [38,39]. This behaviour is typically shown by plastic crystals. For these compounds, the transition from solid to liquid is not as sharp as in other solids. The ions are not as anchored to the lattice as in classical crystalline solids, being free to rotate or vibrate. This makes the entropy of these phases to be high, and as a result, the entropy of melting is small [40]. This state is also understood to contain many lattice vacancies as a result of the rotational disorder, for which the material can present plastic material properties, as high ionic conductivity.

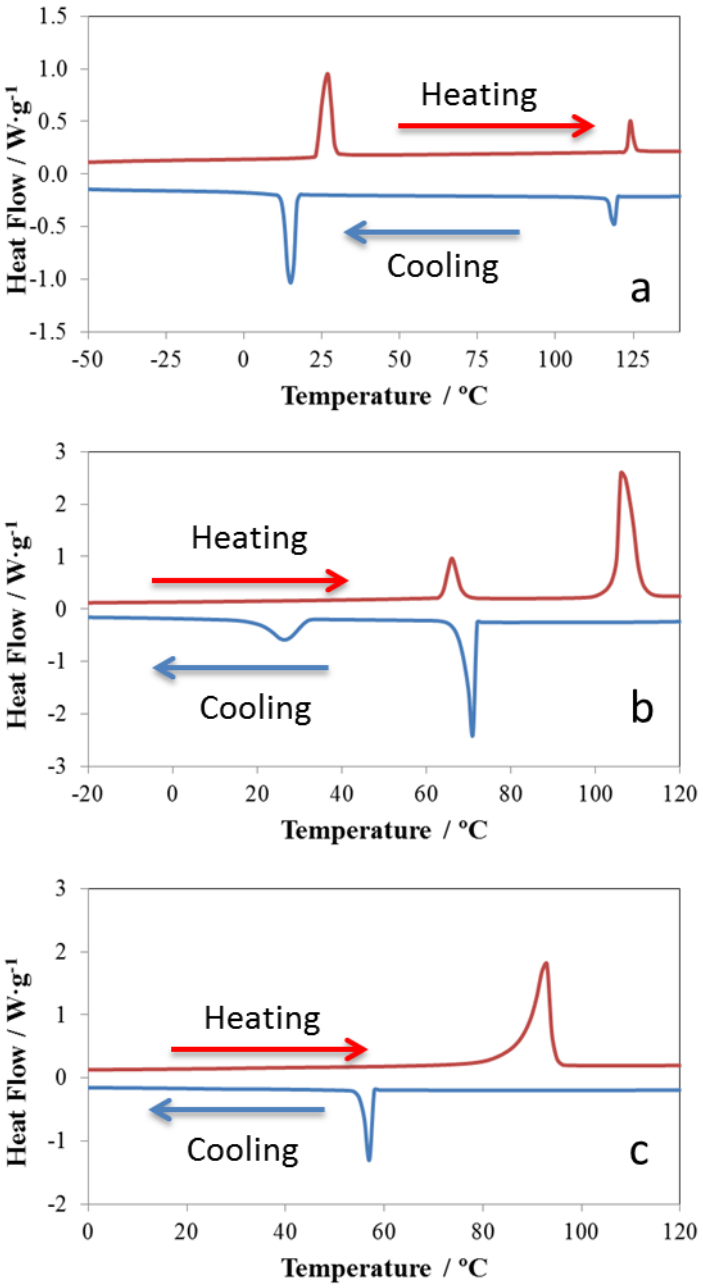

Fig. 1. Cooling (blue) and heating (red) scans of DSC curves (exo down) obtained at 5º C min^{-1} for the three choline based ionic liquids: a) [Chol][H_2PO_4], b) [Chol][Tos], c) [Chol][Ac]

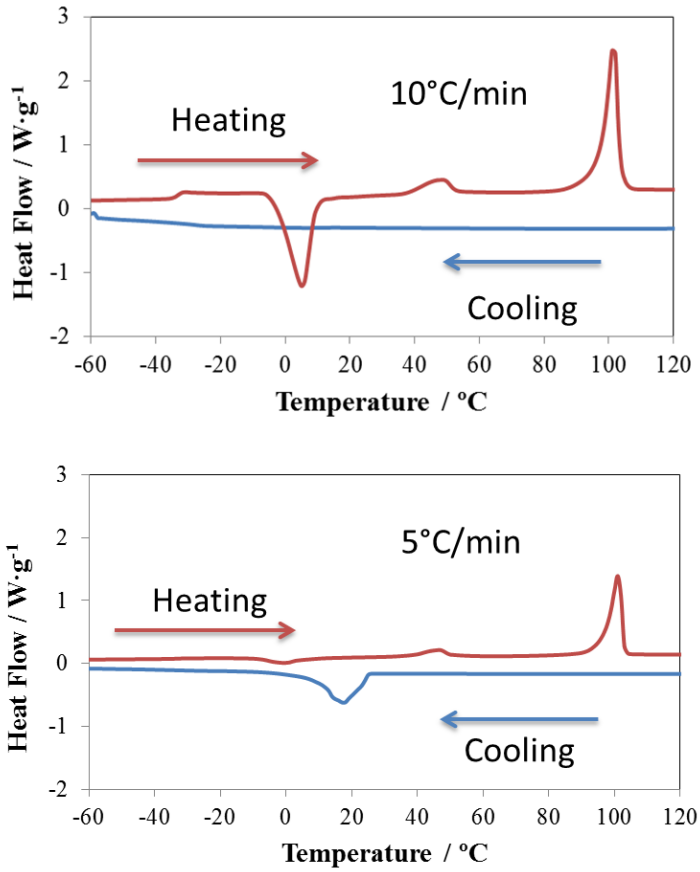

Fig. 2. DSC curves (exo down) of [C_2py][Tos] at different heating rates

Table 2. Melting (t_m), freezing (t_f), glass transition (t_g), solid-solid (t_{ss}) and cold crystallization (t_{cc}) temperatures, enthalpy (ΔH_m) and entropy changes (ΔS_m) of melting of the selected ILs acquired using differential scanning calorimetry (DSC). All temperatures correspond to the onset of the peaks, except for glass transition that corresponds to the midpoint step temperature Experiments were performed with (1008 ± 10) hPa of atmospheric atmosphere, and relative humidity of (55 ± 10)%. Reference data are also included.

IL	t_m / ºC	t_f / ºC	t_g / ºC	t_{cc} / ºC	t_{ss} / ºC	ΔH_m / kJ·mol^{-1}	ΔS_m / J mol^{-1} K^{-1}
[Chol][H_2PO_4]	123	120	---		23	1.3	3.3
	190[36]		22[36]		20/120[36]		
	180[11]				110[11]		
	119[33,34]						
[Chol][Tos]	105	73			66	19.1	51
	107 [28]						
[Chol][Ac]	86	59				17.3	48
	51[22]					8.9 [41]	
	74[30]					16.5 [42]	
	80[18,29]						
	72[21]						
	89 [41]						
	68 [42]						
	75 [31]						
[C_2Py][Tos]	101	--	-33	-3	48	21.0	56

Expanded uncertainties (0.95 level of confidence) U(t)=2ºC, $U_r(\Delta H_m)$= 10%, $U_r(\Delta S_m)$= 10%

The obtained melting entropies for [Chol][Tos], [Chol][Ac] and [C_2Py][Tos] are relatively high compared with salts undergoing plastic crystallization, whose ΔS_m < 20 J mol^{-1} K^{-1} [43], indicating that these ILs present rather a rigid crystalline structure than plastic one. The other studied IL, [Chol][H_2PO_4], is clearly a liquid crystal, as the very low ΔS_m suggests.

Heat capacity analysis

Fig. 3 shows the isobaric specific heat (c_p), for the studied systems between (293.15 and 348.15) K. Samples are in solid phase over the whole studied temperature interval. As usual, c_p increases with temperature. A clear dependence with the anion is observed, as obtained in a previous work [44], being the lowest values corresponding to tosylate based ILs and the highest to that containing acetate anion. In this case, also dependence with cation is observed, being choline ILs those presenting the highest values. Table 3 shows the isobaric molar heat capacities values, C_p, for the selected ILs between (293.15 and 348.15) K. These data are also plotted in Fig. 4. Isobaric molar heat capacity also increases with temperature and follows the tendency:

$$[Chol][\ H_2PO_4] < [Chol][Ac] < [C_2Py][Tos] < [Chol][Tos],$$

C_p often correlates with molecular weight [42], since degrees of freedom of the molecule strongly increase with its size. However, the obtained C_p results show that the studied ILs do not follow this tendency. This deviation from the usually observed behaviour could be related with the ability of the choline and acetate ions to form hydrogen bonds, since it is well known that they revert in an important positive contribution to heat capacity.

For [Chol][Tos], which shows a solid-solid transition in the studied temperature range, larger values for solid II are found, with an increment in heat capacity between the two phases, ΔC_p, around 10 $J \cdot mol^{-1} \cdot K^{-1}$. It is worth to note that the low temperature reported values for [Chol][H_2PO_4] and [C_2Py][Tos] are those of the metastable high temperature solid phase. Although samples were thermostated at 288.15 K for an hour before carrying out the experiments, the stable phase could not be attained, as it was in Q100 experiences. Probably lower temperatures than 288.15 K are needed in order to make these phases to appear.

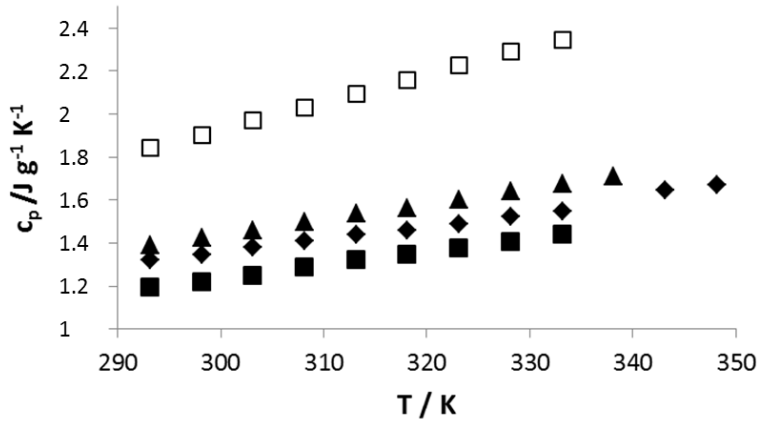

Fig. 3. Isobaric specific heat capacities, c_p for the four ILs: ▲ [Chol][H_2PO_4], ♦[Chol][Tos], □ [Chol][Ac], ■[C_2Py][Tos].

Table 3. Isobaric molar heat capacities of the ILs under atmospheric pressure (990 ± 12) hPa. All these values correspond to sample solid phase.

	C_p/J mol^{-1}K^{-1}			
T /K	[Chol][H_2PO_4]	[Chol][Tos]	[Chol][Ac]	[C_2Py][Tos]
293.15	*279.3	363.2	300.5	*333.7
298.15	286.5	371.3	310.5	*340.1
303.15	293.7	380.2	321.5	*349.2
308.15	301.3	388.0	330.9	*359.1
313.15	309.1	396.2	341.7	*368.5
318.15	314.6	401.8	351.8	*375.4
323.15	322.5	410.1	363.2	384.5
328.15	329.6	419.4	373.3	392.2
333.15	337.2	426.6	382.4	402.5
338.15	344.4			
343.15		452.6		
348.15		460.1		

Standard uncertainties: u(T) = 0.1 K; $u_r(C_p)$ = 2%.

*Corresponds to metastable high-temperature solid phase.

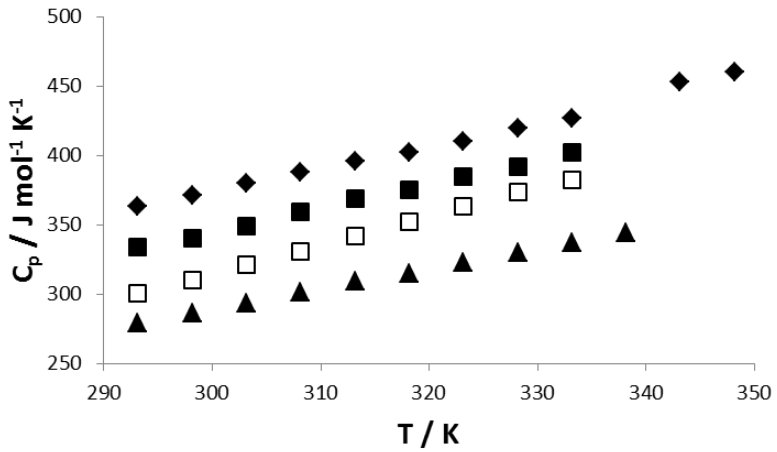

Fig. 4. Isobaric molar heat capacities, C_p for the four ILs: ▲ [Chol][H_2PO_4], ♦[Chol][Tos], □ [Chol][Ac], ■[C_2Py][Tos].

Up to our knowledge no data about this property can be found in literature for the studied ionic liquids. In order to fit isobaric molar heat capacity values with temperature for the ILs, a linear equation is used

$$C_p = A_0 + A_1 T \qquad (1)$$

The values of A_i parameters as well as standard deviation s are given in Table 4.

Table 4. Fitting Coefficients A_i of Eq. (1) and Standard Derivation *s*.

IL	A_0/ J mol^{-1} K^{-1}	A_1/ J mol^{-1} K^{-2}	*s*
[Chol][H_2PO_4]	-143.09	1.4412	0.4
[Chol][Tos] (solid I)	-61.91	1.4993	0.7
[Chol][Tos] (solid II)	-305.46	2.0668	0.5
[Chol][Ac]	-173.99	1.7284	1.0
[C_2Py][Tos]	-140.34	1.4328	0.5

Thermogravimetric analysis

Dynamic study

Fig. 5 shows the TG and DTG curves of the four ILs performed in air and N_2 atmospheres with a heating rate of 10 ºC min^{-1}. Thermal stability parameters determined

from the dynamic TG and DTG curves are summarized in Table 5. Onset temperatures were determined as it was indicated in previous works [32]; weight at onset temperature (W_{onset}) and temperatures of the minima of DTG (t_{peak}) are also presented in this table. Up to our better knowledge, previous literature data of thermal stability of these ionic liquids are scarce. Petkovic *et al*. [29] and Fukaya *et al*. [22] obtained values of 169 ºC and 189 ºC, respectively, for onset temperature of [Chol][Ac], which are in relatively concordance with our results; the differences can be attributed to different experimental conditions and different methods to obtain this parameter from TGA curves. Several authors [11,36] indicate that [Chol][H_2PO_4] is stable up to 200 ºC, agreeing with our results.

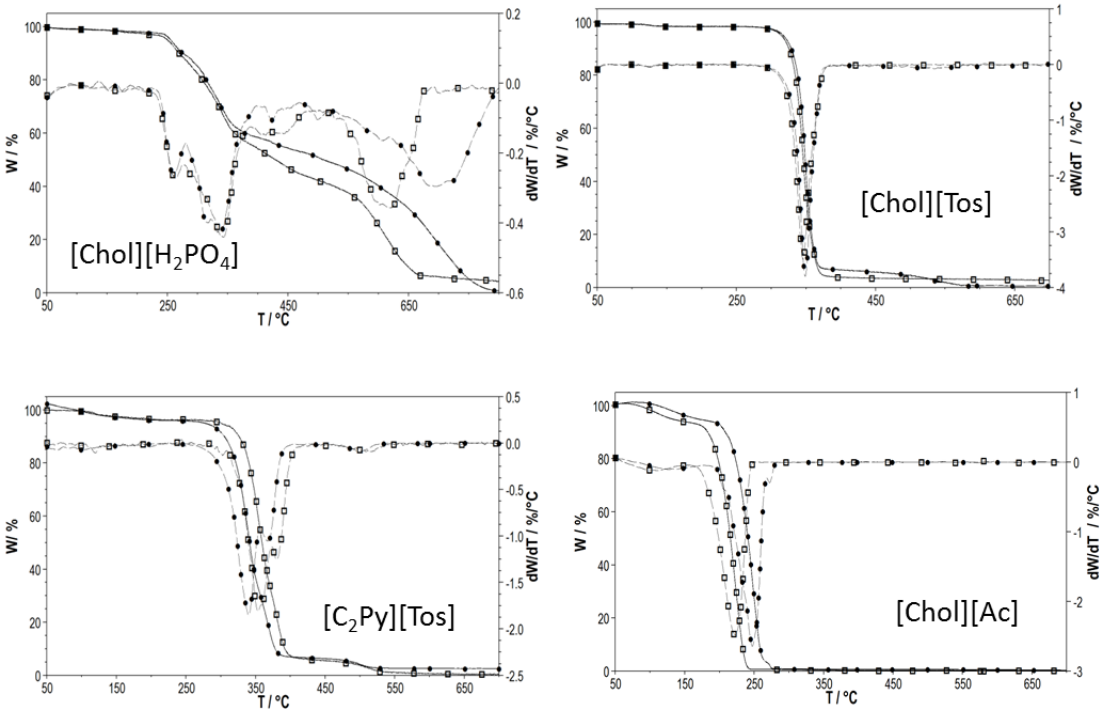

Fig. 5. Dynamic TG (solid) and DTG (dashed) curves of the selected ILs obtained at 10 ºC min^{-1} under air (●) and N_2 (□) atmospheres.

Table 5. Onset temperatures (t_{onset}), sample remaining weight (in %) at onset temperature (W_{onset}) and temperature of the minimum of DTG (t_{peak}) from the dynamic scans (10 ºC min^{-1}) in air and nitrogen atmospheres. Experiments were performed with (1008 ± 10) hPa of atmospheric atmosphere, and relative humidity of (55 ± 10)%.

Ionic Liquid	Atmosphere	t_{onset}/ ºC	W_{onset}/ %	t_{peak}/ ºC
[Chol][H_2PO_4]	Air	247	97	263
		275	91	329
		632	36	695
	Nitrogen	246	97	263
		277	88	335
		570	32	614
[Chol][Tos]	Air	336	82	349
	Nitrogen	332	84	346
[Chol][Ac]	Air	226	83	248
	Nitrogen	200	85	222
[C_2Py][Tos]	Air	316	84	340
	Nitrogen	335	86	357

Expanded uncertainties are U(t) = 8 ºC and U(W) = 2% (0.95 level of confidence (k=2))

In Fig. 6, a comparison between TG curves obtained for the four selected ILs at 10 ºC min^{-1} under both, air (a) and N_2 (b), atmospheres is presented. As it can be observed from this figure, there are different thermal behaviors taking into account the beginning of the mass loss, characterized through the onset temperature, as well as the shape of the TG curves. For example, in case of [Chol][Ac], the TG curve shows a single step (obviating the initial one due to the water and volatiles loss) after which the sample has lost the whole mass. In case of [Chol][Tos] and [C_2Py][Tos] a major decomposition step is recorded followed by a small one where the degradation of the sample ends at high temperatures. For the [Chol][H_2PO_4] the TG curve shows two main, but not well resolved, steps which means that the associated processes are overlaid during the heating of the sample.

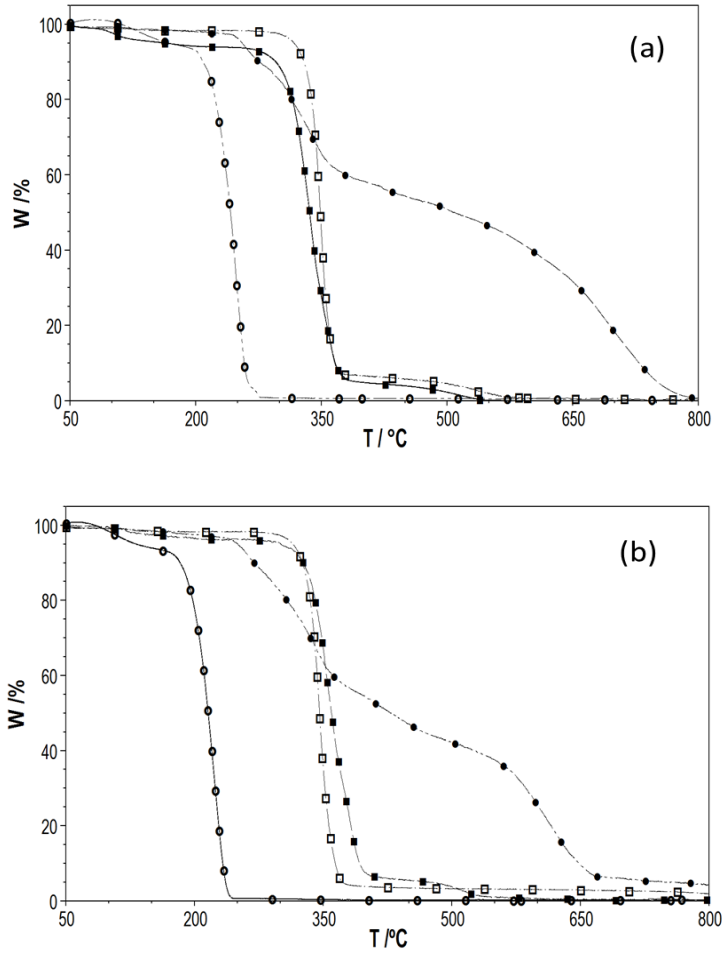

Fig. 6. TG curves obtained under air (a) and N_2 (b) atmospheres of the selected ILs at 10 ºC min^{-1}: ❍[Chol][Ac], □[Chol][Tos], ■[C_2Py][Tos], •[Chol][H_2PO_4].

Although onset temperature cannot be considered as the liquid range upper limit [32,45], it can be used to compare the short-term thermal stability of different ILs. According to this, the following thermal stability trend is obtained:

[Chol][Ac] < [Chol][H_2PO_4] < [C_2Py][Tos] < [Chol][Tos]

These results are in total agreement with previous findings that concluded the main role of anion on the thermal stability [46,47]. Cao *et al.* [48] analyzed the thermal stability of 66 ILs with different anions, among them, $[Ac]^-$, $[H_2PO_4]^-$ and $[Tos]^-$, with different cations, obtaining similar trends than us.

Isothermal study

Taking into account the small differences between the dynamic stability results obtained in both selected atmospheres, the isothermal analysis was only performed in air.

Fig. 7 shows the isothermal scans at different temperatures (all of them lower than t_{onset}) in air atmosphere for the four ILs.

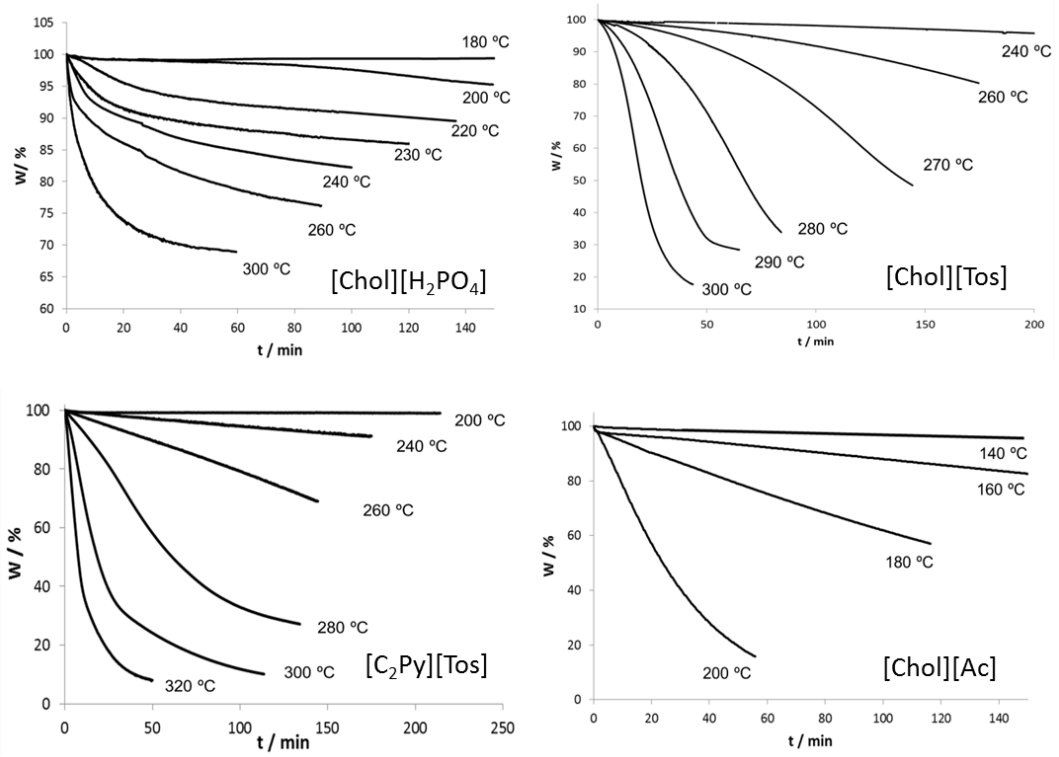

Fig. 7. Isothermal scans in air atmosphere at different temperatures for the four ILs. All experiments were performed at atmospheric pressure of 998 ± 12 hPa

As it was expected, in all cases there is a significant mass loss in short times after exposing the sample at temperatures lower than onset one. [Chol][Ac] is the less stable, as it was also concluded in the dynamic study. For the other three ILs, a sequence can be stablished making a comparison of one of the isothermal scans. Thus, for isothermal experiments at 260 °C it can be seen that a degradation of 10% is observed for the [Chol][H_2PO_4] after 7 min of exposition, whereas to get the same mass loss, 50 and 115 min were necessary in case of [C_2Py][Tos] and [Chol][Tos], respectively. That indicates, once again, the strong influence of the anion on the thermal stability of ionic

liquids. Therefore, according to this isothermal degradation study, the following sequence for the thermal stability can be stablished:

$$[Chol][Ac] << [Chol][H_2PO_4] < [C_2Py][Tos] < [Chol][Tos],$$

which is the same obtained through the dynamic analysis.

Kinetics of isothermal degradation

The kinetics of mass loss for the selected ILs was analysed from isothermal TGA results following the methodology reported in previous articles [27,45]. The Arrhenius equation is a good tool to analyse the temperature dependence on the mass loss rate, *k*:

$$k = A\,exp\left(\frac{-E_a}{RT}\right) \quad (2)$$

where E_a is the activation energy and A is the pre-exponential coefficient. This relation allows the prediction of the decomposition rate at any temperature.
By defining the degree of conversion, α, as:

$$\alpha = \frac{m_0 - m}{m_0 - m_\infty} \quad (3)$$

where m is the measured experimental mass at temperature T, m_0 the initial mass, and m_∞ the mass at the end of the non-isothermal experiments and considering the rate of conversion $d\alpha/dt$, the k constant is obtained as the slope of a linear fitting of conversion rate versus time for each isothermal scan.

From the linear relation between ln k and temperature (Fig. 8) the activation energy of the thermal degradation process is calculated for each IL, which is presented, together with the preexponential factor in Table 6.

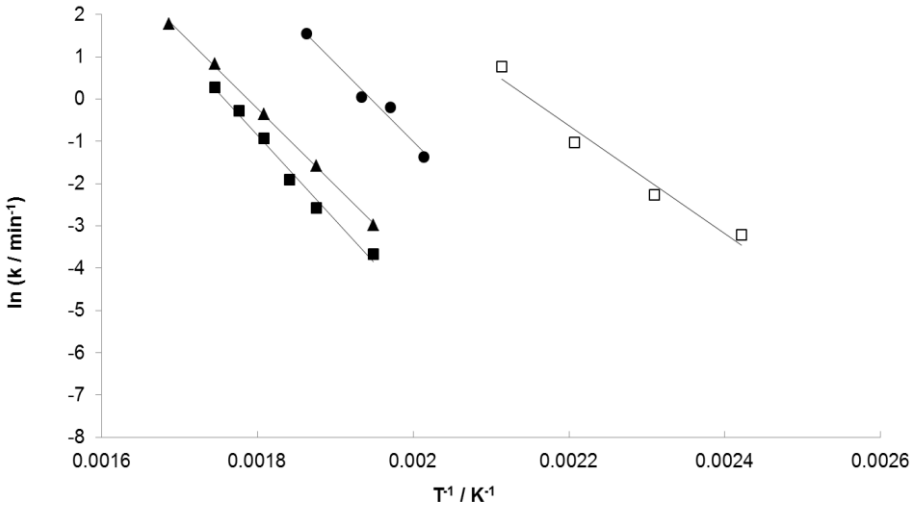

Fig. 8. Arrhenius plots for the selected ILs: •[Chol][H_2PO_4], ■[Chol][Tos], □[Chol][Ac], ▲[C_2Py][Tos].

Table 6. Activation energies, E_a with the standard uncertainty, ΔE_a and pre-exponential coefficients, A, for the four ILs obtained from the Arrhenius equation (1).

Ionic Liquid	$E_a \pm \Delta E_a$ / kJ mol^{-1}	A / min^{-1}	R^2
[Chol][H_2PO_4]	154± 18	4.64 10^{15}	0.974
[Chol][Tos]	167± 9	2.04 10^{15}	0.987
[Chol][Ac]	106± 14	8.23 10^{11}	0.967
[C_2Py][Tos]	151± 2	1.25 10^{14}	0.999

These values of activation energy are in good concordance with the obtained from Cao *et al.* [48] for different ILs with similar anions, except in the case of [H_2PO_4] based IL, but this disagreement can be attributed to differences in the temperature interval. [Chol][Ac] presents the lowest values of activation barrier and degradation temperature in this oxidative atmosphere, whereas the opposite situation corresponds to [Chol][Tos] which shows the highest values of both, activation energy and temperature of degradation. Thus, from these energy values, the observed tendency agrees with that resulted from dynamic and isothermal values:

[Chol][Ac] < [C_2Py][Tos] ≈ [Chol][H_2PO_4] < [Chol][Tos]

Maximum operation temperature (MOT)

The level of degradation allowed in different applications is not yet clear in literature, ranging from 1% in one year [49] to 10% in 10 h [50]. In this work, an estimation of the maximum operation temperature (MOT) for the four ILs has been done following the criteria of Seeberger *et al.*[49]. They proposed the use of the following equation to calculate the MOT for a defined time of operation (t_{max}):

$$MOT = \frac{{}^{Ea}/_{R}}{4.6+ln(A+t_{max})} \quad (4)$$

where R is the gas constant.

In Fig. 9, the MOT (in Celsius degrees) is depicted versus the operating time (in hours) for the four studied ILs.

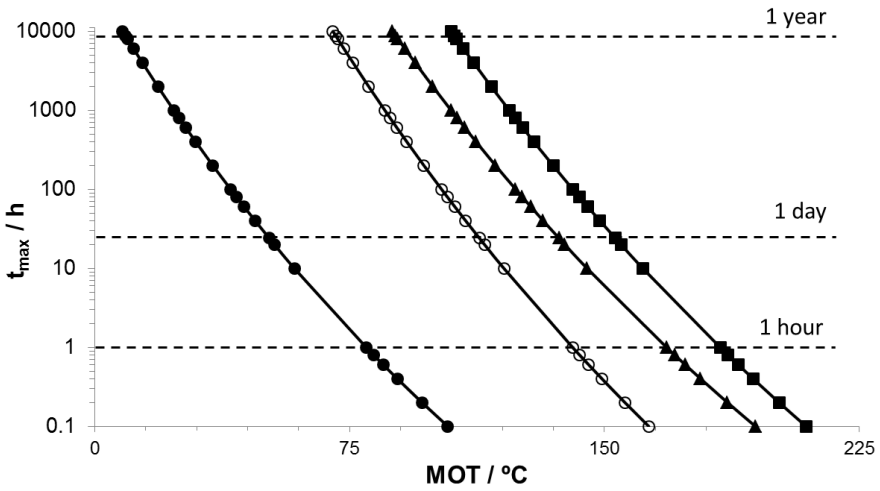

Fig. 9. Calculation of the maximum operation temperature (MOT) in air atmosphere of the four selected ILs: • [Chol][Ac]. ○ [Chol][H_2PO_4]. ▲ [C_2Py][Tos] and ■[Chol][Tos], depending on the operating time.

As expected, temperature decreases systematically with the exposure time. Hence, following this criterion, the MOT for the IL [Chol][Tos] changes from almost 200 ºC for 1 h. to 160 ºC for 1 day and to 110 ºC for 1 year (8000 h) of operation times; whereas for [Chol][Ac] temperature cannot exceed 50 ºC to guaranty the quality of the IL during 1 day (24 h). So it can be said that this MOT study ratifies that concluded from the above thermal stability studies, obtaining a similar trend than those presented before:

$$[Chol][Ac] < [Chol][H_2PO_4] < [C_2Py][Tos] < [Chol][Tos]$$

Thermal stability trends obtained through different criteria, *i.e.* according to onset temperatures (from dynamic experiments), to energy, and to MOT values (isothermal studies), were very similar, a fact that avails the reliability of the used methodologies.

Conclusions

Phase transitions, isobaric heat capacities and thermal stability of four ionic liquids (ILs) with application in energy field were determined in this work.

Main results are the following:

The four studied ILs showed crystalline behaviour, with melting temperatures ranging from 86ºC to 123ºC. According to ΔS_m values, a rigid crystalline structure would be associated to the [Chol][Tos], [Chol][Ac] and $[C_2Py][Tos]$ ionic liquids (ΔS_m >20 J K^{-1} mol^{-1}) whereas $[Chol][H_2PO_4]$ shows plastic crystal behaviour (ΔS_m <20 J K^{-1} mol^{-1}).

Heat capacities were measured in the temperature interval between (293.15 and 348.15) K being all the samples in solid phase. This property increased with temperature. Isobaric molar heat capacity also increases with temperature and follows the tendency:

$$[Chol][H_2PO_4] < [Chol][Ac] < [C_2Py][Tos] < [Chol][Tos]$$

A clear dependence with the anion is observed for both, heat capacities and thermal stability, being ILs with the tosylate anion those that presented the highest values of molar heat capacities and the highest thermal stability.

Thermal stability trends obtained through different criteria, *i.e.* according to onset temperatures, to activation energy, and to maximum operation temperature (MOT) values, were very similar. As it can be expected, this property was strongly dependent of the anion, presenting the [Ac] and the [Tos] based IL the lowest and the highest thermal stability, respectively.

Acknowledgements

Authors acknowledge M. Gómez (RIAIDT-USC) for the technical support in DSC measurements. This work was supported by Spanish Ministry of Economy and Competitiveness and FEDER Program through the projects MAT2017-89239-C2-1-P and FIS2017-89361-C3- 3-P, as well as by Xunta de Galicia through GRC ED431C 2016/001 and ED431E 2018/08 projects and the Galician Network of Ionic Liquids (ReGaLIs) ED431D 2017/06.

References

[1] N. V Plechkova, K.R. Seddon, Applications of ionic liquids in the chemical industry., Chem. Soc. Rev. 37 (2008) 123–150. doi:10.1039/b006677j.

[2] J. Ma, X. Hong, Application of ionic liquids in organic pollutants control, J. Environ. Manage. 99 (2012) 104–109. doi:10.1016/j.jenvman.2012.01.013.

[3] T. Greaves, C. Drummond, Protic ionic liquids: properties and applications, Chem. Rev. 108 (2008) 206–37. doi:10.1021/cr068040u.

[4] M. Cvjetko Bubalo, S. Vidović, I. Radojčić Redovniković, S. Jokić, Green solvents for green technologies, J. Chem. Technol. Biotechnol. 90 (2015) 1631–1639. doi:10.1002/jctb.4668.

[5] S. Studzinska, B. Buszewski, Study of toxicity of imidazolium ionic liquids to watercress (Lepidium sativum L.), Anal. Bioanal. Chem. 393 (2009) 983–990. doi:10.1007/s00216-008-2523-9.

[6] B.D. Ribeiro, M.A.Z. Coelho, L.P.N. Rebelo, I.M. Marrucho, Ionic liquids as additives for extraction of saponins and polyphenols from mate (ilex paraguariensis) and tea (camellia sinensis), Ind. Eng. Chem. Res. 52 (2013) 12146–12153. doi:10.1021/ie400529h.

[7] D.M. Foureau, R.M. Vrikkis, C.P. Jones, K.D. Weaver, D.R. Macfarlane, J.C. Salo, I.H. Mckillop, G.D. Elliott, In vitro assessment of choline dihydrogen phosphate (CDHP) as a vehicle for recombinant human interleukin-2 (rhIL-2), Cell. Mol. Bioeng. 5 (2012) 390–401. doi:10.1007/s12195-012-0243-x.

[8] B.L. Gadilohar, G.S. Shankarling, Choline based ionic liquids and their applications in organic transformation, J. Mol. Liq. 227 (2017) 234–261.

doi:10.1016/j.molliq.2016.11.136.

[9] L. Tanzi, M. Nardone, P. Benassi, F. Ramondo, R. Caminiti, L. Gontrani, Choline salicylate ionic liquid by X-ray scattering, vibrational spectroscopy and molecular dynamics, J. Mol. Liq. 218 (2016) 39–49. doi:10.1016/j.molliq.2016.02.020.

[10] S. Aparicio, M. Atilhan, A computational study on choline benzoate and choline salicylate ionic liquids in the pure state and after CO 2 adsorption, J. Phys. Chem. B. 116 (2012) 9171–9185. doi:10.1021/jp304755k.

[11] P. Barbosa, J.M. Campos, A. Turygin, V. Shur, A. Kholkin, A.M.M.V.B. Timmons, F.M. Figueiredo, Piezoelectric poly(lactide) stereocomplexes with a cholinium organic ionic plastic crystal, J. Mater. Chem. C. (2017) 12134–12142. doi:10.1039/C7TC03484A.

[12] J.N. Pendleton, B.F. Gilmore, The antimicrobial potential of ionic liquids: A source of chemical diversity for infection and biofilm control, Int. J. Antimicrob. Agents. 46 (2015) 131–139. doi:10.1016/j.ijantimicag.2015.02.016.

[13] R. Moulton, Ionic liquids containing borate or phosphate anions, WO 2004/005222, 2004. doi:10.1016/s0026-0576(04)84713-5.

[14] R. Klein, M. Kellermeier, D. Touraud, E. Müller, W. Kunz, Journal of Colloid and Interface Science Choline alkylsulfates – New promising green surfactants, J. Colloid Interface Sci. 392 (2013) 274–280. doi:10.1016/j.jcis.2012.10.003.

[15] S.H. Zeisel, K.A. Da Costa, Choline: An essential nutrient for public health, Nutr. Rev. 67 (2009) 615–623. doi:10.1111/j.1753-4887.2009.00246.x.

[16] S.H. Zeisel, A brief history of choline, Ann. Nutr. Metab. 61 (2012) 254–258. doi:10.1159/000343120.

[17] H. Zhao, G.A. Baker, S. Holmes, New eutectic ionic liquids for lipase activation and enzymatic preparation of biodiesel, Org. Biomol. Chem. 9 (2011) 1908. doi:10.1039/c0ob01011a.

[18] Q. Zhang, M. Benoit, K. Dea Oliveira Vigier, J. Barrault, F. Jérŏme, Green and inexpensive choline-derived solvents for cellulose decrystallization, Chem. - A Eur. J. 18 (2012) 1043–1046. doi:10.1002/chem.201103271.

[19] P.B. Sánchez, J. García, J. Salgado, E. González-Romero, Studies of Volumetric and Transport Properties of Ionic Liquid-Water Mixtures and Its Viability to Be Used in Absorption Systems, ACS Sustain. Chem. Eng. 4 (2016). doi:10.1021/acssuschemeng.6b01541.

[20] U.A. Rana, R. Vijayaraghavan, D.R. MacFarlane, M. Forsyth, Plastic crystal phases with high proton conductivity, J. Mater. Chem. 22 (2012) 2965–2974. doi:10.1039/C2JM15288F.

[21] N. Muhammad, M.I. Hossain, Z. Man, M. El-Harbawi, M.A. Bustam, Y.A. Noaman, N.B. Mohamed Alitheen, M.K. Ng, G. Hefter, C.Y. Yin, Synthesis and physical properties of choline carboxylate ionic liquids, J. Chem. Eng. Data. 57 (2012) 2191–2196. doi:10.1021/je300086w.

[22] Y. Fukaya, Y. Iizuka, K. Sekikawa, H. Ohno, Bio ionic liquids: room temperature ionic liquids composed wholly of biomaterials, Green Chem. 9 (2007) 1155. doi:10.1039/b706571j.

[23] J.J. Parajó, M. Villanueva, P.B. Sánchez, J. Salgado, Liquid window of some biologically-active ionic liquids, J. Chem. Thermodyn. 126 (2018) 1–10. doi:10.1016/j.jct.2018.06.014.

[24] J. Salgado, J.J. Parajó, M. Villanueva, J.R. Rodríguez, O. Cabeza, L.M. Varela, Liquid range of ionic liquid – Metal salt mixtures for electrochemical applications, J. Chem. Thermodyn. 134 (2019) 164–174. doi:10.1016/j.jct.2019.03.012.

[25] M. Zabransky, V. Ruzicka, E.S. Domalski, Heat Capacity of Liquids: Critical Review and Recommended Values, J. Phys. Chem. Ref. Data. 24 (2001) 1199–1689. doi:10.1515/ci.2002.24.3.21c.

[26] J.J. Parajó, M. Villanueva, I. Otero, J. Fernández, J. Salgado, Thermal stability of aprotic ionic liquids as potential lubricants. Comparison with synthetic oil bases, J. Chem. Thermodyn. 116 (2018) 185–196. doi:https://doi.org/10.1016/j.jct.2017.09.010.

[27] J. Salgado, J.J. Parajó, J. Fernández, M. Villanueva, Long-term thermal stability of some 1-butyl-1-methylpyrrolidinium ionic liquids, J. Chem. Thermodyn. 74 (2014) 51–57.

[28] G. Wandelt, G. Heilner, A process for the preparation of salts of quaternary ammonium bases, DE571294C, 1933.

[29] M. Petkovic, J.L. Ferguson, H.Q.N. Gunaratne, R. Ferreira, M.C. Leitão, K.R. Seddon, L.P.N. Rebelo, C.S. Pereira, Novel biocompatible cholinium-based ionic liquids—toxicity and biodegradability, Green Chem. 12 (2010) 643. doi:10.1039/b922247b.

[30] S. Koda, H. Takayama, T. Shibata, T. Mori, S. Kojima, I.-S. Park, T.-G. Shin, Small angle neutron scattering study on the structural variation of lysozyme in bioprotectants, J. Korean Phys. Soc. 66 (2015) 1376–1380. doi:10.3938/jkps.66.1376.

[31] T. Brünig, K. Krekić, C. Bruhn, R. Pietschnig, Calorimetric Studies and Structural Aspects of Ionic Liquids in Designing Sorption Materials for Thermal Energy Storage, Chem. - A Eur. J. 22 (2016) 16200–16212. doi:10.1002/chem.201602723.

[32] M. Villanueva, J.J. Parajó, P.B. Sánchez, J. García, J. Salgado, Liquid range temperature of ionic liquids as potential working fluids for absorption heat pumps, J. Chem. Thermodyn. 91 (2015) 127–135. doi:10.1016/j.jct.2015.07.034.

[33] D. Hekmat, D. Hebel, D. Weuster-Botz, Crystalline proteins as an alternative to standard formulations, Chem. Eng. Technol. 31 (2008) 911–916. doi:10.1002/ceat.200800038.

[34] J.M. Lopes, F.A. Sánchez, S.B.R. Reartes, M.D. Bermejo, Á. Martín, M.J. Cocero, Melting point depression effect with CO2in high melting temperature cellulose dissolving ionic liquids. Modeling with group contribution equation of state, J. Supercrit. Fluids. 107 (2016) 590–604. doi:10.1016/j.supflu.2015.07.021.

[35] K. Fujita, D.R. MacFarlane, K. Noguchi, H. Ohno, Choline dihydrogen phosphate, Acta Crystallogr. Sect. E Struct. Reports Online. 65 (2009). doi:10.1107/S1600536809007259.

[36] U.A. Rana, P.M. Bayley, R. Vijayaraghavan, P. Howlett, D.R. MacFarlane, M. Forsyth, Proton transport in choline dihydrogen phosphate/H3PO4 mixtures, Phys. Chem. Chem. Phys. 12 (2010) 11291. doi:10.1039/c0cp00156b.

[37] D. Hekmat, D. Hebel, S. Joswig, M. Schmidt, D. Weuster-Botz, Advanced

protein crystallization using water-soluble ionic liquids as crystallization additives, Biotechnol. Lett. 29 (2007) 1703–1711. doi:10.1007/s10529-007-9456-9.

[38] L. Jin, K.M. Nairn, C.M. Forsyth, A.J. Seeber, D.R. Macfarlane, P.C. Howlett, M. Forsyth, J.M. Pringle, Structure and Transport Properties of a Plastic Crystal Ion Conductor : Diethyl (methyl)(isobutyl) phosphonium Hexa fl uorophosphate-SI, J. Am. Chem. Soc. (2012) 1–6. doi:10.1021/ja301175v.

[39] D.R. MacFarlane, P. Meakin, J. Sun, N. Amini, M. Forsyth, Pyrrolidinium Imides. A New Family of Molten Salts and Conductive Plastic Crystal Phases, J. Phys. Chem. B. 103 (1999) 4164–4170. doi:10.1021/jp984145s.

[40] P. Wasserscheid, T. Welton, Ionic liquids in Synthesis, Wiley -VCH Verlag, Weinheim, 2003.

[41] L. Fernandez, L.P. Silva, M.A.R. Martins, O. Ferreira, J. Ortega, S.P. Pinho, J.A.P. Coutinho, Indirect assessment of the fusion properties of choline chloride from solid-liquid equilibria data, Fluid Phase Equilib. 448 (2017) 9–14. doi:10.1016/j.fluid.2017.03.015.

[42] J.M. Lopes, A.B. Paninho, M.F. Môlho, A.V.M. Nunes, A. Rocha, N.M.T. Lourenço, V. Najdanovic-Visak, Biocompatible choline based ionic salts: Solubility in short-chain alcohols, J. Chem. Thermodyn. 67 (2013) 99–105. doi:10.1016/j.jct.2013.07.025.

[43] K. Machanová, Z. Wagner, A. Andresova, J. Rotrekl, A. Boisset, J. Jacquemin, M. Bendova, Thermal properties of alkyl-triethylammonium bis {(trifluoromethyl)sulfonyl}imide ionic liquids, J. Solution Chem. 44 (2015) 790–810. doi:10.1007/s10953-015-0323-3.

[44] J. Salgado, T. Teijeira, J.J. Parajó, J. Fernández, J. Troncoso, Isobaric heat capacity of nanostructured liquids with potential use as lubricants, J. Chem. Thermodyn. 123 (2018). doi:10.1016/j.jct.2018.03.031.

[45] J.J. Parajó, M. Villanueva, I. Otero, J. Fernández, J. Salgado, Thermal stability of aprotic ionic liquids as potential lubricants. Comparison with synthetic oil bases, J. Chem. Thermodyn. 116 (2018). doi:10.1016/j.jct.2017.09.010.

[46] M. Lorenzo, M. Vilas, P. Verdía, M. Villanueva, J. Salgado, E. Tojo, Long-term

thermal stabilities of ammonium ionic liquids designed as potential absorbents of ammonia, RSC Adv. 5 (2015). doi:10.1039/c5ra03192c.

[47] C. Maton, N. De Vos, C. V. Stevens, Ionic liquid thermal stabilities: decomposition mechanisms and analysis tools, Chem. Soc. Rev. 42 (2013) 5963–5977. doi:10.1039/c3cs60071h.

[48] Y. Cao, T. Mu, Comprehensive Investigation on the Thermal Stability of 66 Ionic Liquids by Thermogravimetric Analysis, Ind. Eng. Chem. Res. 53 (2014) 8651–8664.

[49] A. Seeberger, A.-K. Andresen, A. Jess, Prediction of long-term stability of ionic liquids at elevated temperatures by means of non-isothermal thermogravimetrical analysis., Phys. Chem. Chem. Phys. 11 (2009) 9375–81. doi:10.1039/b909624h.

[50] R. Liang, M. Yang, X. Xuan, Thermal stability and thermal decomposition kinetics of 1-butyl-3-methylimidazolium dicyanamide, Chinese J. Chem. Eng. 18 (2010) 736–741. doi:10.1016/S1004-9541(09)60122-1.